Modern Imaging of Pituitary Adenomas

Waiel Bashari MSc MRCP(UK)[1]*, Russell Senanayake MSc MRCP(UK)[1]*, Antía Fernández-Pombo MD[1,2]*, Daniel Gillett MSc[3], Olympia Koulouri MRCP(UK)[1], Andrew S Powlson MRCP(UK)[1], Tomasz Matys PhD FRCR[4], Daniel Scoffings FRCR[4], Heok Cheow FRCR[3,4], Iosif Mendichovszky PhD FRCR[3,4], Mark Gurnell PhD FRCP[1]

Cambridge Endocrine Molecular Imaging Group, [1]Metabolic Research Laboratories, Wellcome Trust-MRC Institute of Metabolic Science, and Departments of [3]Nuclear Medicine and [4]Radiology, University of Cambridge and National Institute for Health Research Cambridge Biomedical Research Centre, Addenbrooke's Hospital, Hills Road, Cambridge, UK, CB2 0QQ; [2]Division of Endocrinology and Nutrition, University Clinical Hospital of Santiago de Compostela, Spain.

WB*, RS* and AF-P* contributed equally to the manuscript.

Abbreviated title: Modern Pituitary Imaging

Word count: abstract 139; text 3510 (excluding references); tables 3; figures 9.

Corresponding author: Professor M Gurnell, Metabolic Research Laboratories, Wellcome Trust-MRC Institute of Metabolic Science, University of Cambridge, Box 289, Addenbrooke's Hospital, Hills Road, Cambridge, CB2 0QQ, UK; Tel +44-1223-348739; Fax +44-1223-330598; E-mail **mg299@medschl.cam.ac.uk**

Funding: This work was supported by the UK NIHR Cambridge Biomedical Research Centre (WB, OK, ASP, IM, MG)

Abstract

Decision-making in pituitary disease is critically dependent on high quality imaging of the sella and parasellar region. Magnetic resonance imaging (MRI) is the investigation of choice and, for the majority of patients, combined T1 and T2 weighted sequences provide the information required to allow surgery, radiotherapy (RT) and/or medical therapy to be planned and long-term outcomes to be monitored. However, in some cases standard clinical MR sequences are indeterminate and additional information is needed to help inform the choice of therapy for a pituitary adenoma (PA). This article reviews current recommendations for imaging of PA, examines the potential added value that alternative MR sequences and/or CT can offer, and considers how the use of functional/molecular imaging might allow definitive treatment to be recommended for a subset of patients who would otherwise be deemed unsuitable for (further) surgery and/or RT.

Key Words: pituitary, MRI, CT, PET, functional imaging, molecular imaging

Introduction

Although almost always benign, pituitary adenomas (PA) can be associated with significant morbidity and even increased mortality by virtue of hormone hypersecretion (e.g. acromegaly, Cushing syndrome), hypopituitarism, and local mass effects (e.g. visual loss due to chiasmal compression). Recent studies indicate a prevalence rate that is 3.5 to 5-times higher than previously suspected, with clinically-apparent tumours affecting between 1:1000 and 1:1500 of the general population(1). It is possible this still represents an under-estimate bearing in mind up to 14.4% (in autopsy studies) and up to 22.5% (in radiologic studies) of the population have been reported to have a pituitary abnormality, but not all of these undergo formal endocrine assessment(2).

In recent years, the repertoire of medical therapies available for the management of pituitary tumours has increased significantly [e.g. the advent of GH receptor (GHR) antagonist or 2nd generation somatostatin receptor ligand (SRL) therapy for acromegaly](3). In addition, modern radiotherapy techniques (including stereotactic radiosurgery) allow for more precise targeting of a pituitary adenoma while sparing surrounding structures. However, for many patients pituitary surgery remains an important, often first, step in their management (either with curative intent or to reduce tumour bulk and facilitate more effective adjunctive treatment). Good quality imaging of the sella and parasellar regions is therefore critical to decision-making, even when surgery and/or radiotherapy are not recommended. For most patients, this means undergoing dedicated pituitary magnetic resonance (MR) imaging (MRI), which provides important information about the adenoma itself and key surrounding structures. In a small number of cases, pituitary computed tomography (CT) is required (most commonly when MRI is not possible/tolerated). However, while MRI and/or CT provide sufficient information for the management of the majority of cases, routine clinical sequences do not always reliably identify the site of *de novo*, persistent or recurrent adenoma, which in turn may reduce the opportunity for curative surgery and/or radiotherapy (RT).

Accordingly, several groups have explored the potential utility of using alternative MR sequences to inform the management of different pituitary tumour subtypes. In addition, we and others have examined the role(s) of functional imaging (e.g. using molecular PET tracers), in combination with MRI, to allow more accurate localisation of the site(s) of PA. This article provides an update on current approaches to imaging in pituitary adenomas, reviews possible indications for adopting specific MR (and/or CT) sequences and considers how advances in molecular PET imaging might be used to improve patient outcomes from targeted therapies such as (repeat) transsphenoidal surgery (TSS) or stereotactic radiosurgery (SRS).

Magnetic Resonance Imaging

MRI is the preferred cross-sectional imaging modality for identifying lesions within the pituitary gland and surrounding parasellar region, and provides a high detection accuracy(4–6). When requesting a pituitary MR scan, several factors should be taken into account (Table 1).

Insert Table 1 here

The normal anterior pituitary gland is isointense to grey matter on non-contrast T1 and T2 weighted standard Spin Echo (SE) sequences (Fig. 1a,b,e,f), while the posterior pituitary has intrinsic high T1 signal (Fig. 1b) but is hypointense on T2. Following contrast injection, the infundibulum and gland progressively enhance (Fig. 1c,d); however, contrast uptake by pituitary adenomas is typically slower, giving rise to delayed enhancement and washout characteristics, which can help to reveal an otherwise poorly visualised microadenoma (Fig. 2a). Gadolinium, a naturally-occurring lanthanide, is the most commonly employed contrast agent during pituitary imaging. It is particularly suited for use as an MRI contrast agent because it has seven unpaired electrons which confer strong paramagnetic properties. In its free form Gadolinium is toxic and it must therefore be chelated to a carrier ligand to allow clinical use. Gadolinium-based contrast agents (GBCAs) can be divided in to four groups according to whether the carrier ligand is linear or macrocyclic and ionic or non-ionic. In recent years concern has been raised regarding the safety of GBCAs, and the pituitary community has been alerted to the potential for long-term central nervous system retention even in patients with normal renal function, which is particularly relevant given the need for many pituitary patients to continue with long-term imaging surveillance(7). Macrocyclic GBCAs exhibit greater chemical stability than their linear counterparts, and this has been linked to a lower risk of nephrogenic systemic fibrosis and reduced gadolinium tissue deposition; however, they appear to carry a higher risk of allergic reactions, albeit still

relatively rare. Therefore, while GBCAs continue to play an important role in imaging of the sella and parasellar region, it is important to consider when contrast might not be required [e.g. when T1 non-contrast and/or T2 sequences alone can provide sufficient information to inform management (see below)], thereby minimising exposure(8).

Insert Figure 1 here

Another important consideration when imaging the sella is the choice of magnetic field strength. 1.5T SE MRI is still commonly used in routine clinical practice and provides reasonable spatial resolution to permit 2.0 mm or 3.0 mm slice thickness. However, very small microadenomas (e.g. Cushing, thyrotropinoma) may escape detection, although this risk can be partially mitigated by careful selection of the T1 SE parameters(9). In recent years, higher field strength MRI systems (3T and more latterly 7T) have become available, providing higher signal to noise ratio with a reduction in acquisition time, and allowing 1.0 mm sections to be performed(10–12). Therefore, while 1.5T SE MRI is a reasonable option in the first instance, for those patients with suspected microadenomas but with equivocal or 'negative' 1.5T scans, referral for a 3T study should be considered(13). However, it remains to be seen whether using 7T MRI brings sufficient additional benefits to outweigh potential challenges such as the identification of a greater number of incidental pituitary abnormalities.

In routine clinical practice, most PA are readily visualised on T1 and T2 weighted MRI which provide important information about the size of the lesion [micro- (<1cm) versus macro- (≥1cm) adenoma] and the degree of parasellar involvement (Fig. 2). Several approaches have been proposed to define the extent of lateral extension and cavernous sinus invasion, with the most commonly used being the Knosp classification(14). As a general rule, the higher the grade, the greater the degree of cavernous sinus involvement, and the lower the probability of achieving full surgical remission. The inclusion of Grades 3A and 3B

differentiates between the different outcomes for adenomas invading the superior and the inferior cavernous sinus compartments (Fig. 2d)(15).

Insert Figure 2 here

Dynamic contrast-enhanced MRI (based on T1 weighted images obtained pre-and immediately following gadolinium injection) (Table 1) may be indicated when standard sequences have failed to identify a pituitary lesion but clinical features strongly suggest the presence of an adenoma, for example in suspected Cushing disease due to an ACTH-secreting microadenoma(5,16). However, gradient echo [e.g. spoiled gradient echo (SGE) / (fast) spoiled gradient recalled echo (FSPGR/SPGR)] has been reported to offer greater sensitivity for detecting corticotroph microadenomas with only occasional cases detected on dynamic but not gradient echo MRI(16). Strategies such as the administration of corticotrophin-releasing hormone immediately prior to scanning have not provided convincing evidence of an additional benefit(13).

Recently, there has been a resurgence of interest in the potential added value that T2 sequences can offer when assessing pituitary lesions – in particular, offering diagnostic insights that are not deducible from T1 sequences, and also potentially sparing the need for contrast enhanced imaging in some patients (thus reducing GBCA exposure – see above). Jean-François Bonneville has elegantly made the case for increased use (and reporting in the literature) of T2 MR findings in several pituitary disorders, and these are summarised in Table 2(8).

Insert Table 2 here

An array of alternative MR sequences, which are routinely employed in other clinical contexts, have also been tried in several pituitary disorders with mixed results (Table 3).

Although several have shown potential promise, for the most part findings need confirmation in larger cohorts before they can be recommended for routine clinical use.

Insert Table 3 here

Computed tomography (CT)

Modern computed tomography (CT) is a reasonable substitute where MRI is contraindicated (including in patients with non-MR compatible pacemakers/cardiac devices, vascular clips or metallic foreign bodies) or when the patient declines MRI (e.g. due to claustrophobia). Reasonable evaluation of pituitary macroadenomas is possible with dedicated pituitary CT (Fig. 3a), but it is generally less informative for the assessment/detection of small tumours, although advanced CT techniques (e.g. dynamic contrast-enhanced multisection CT) have been trialled and may even aid the detection of conventional MR imaging-occult pituitary microadenomas(17).

Even when MRI is possible, there are several situations in which CT can provide useful additional information regarding a sella-based or parasellar lesion. These include identification of bone destruction (e.g. by an invasive macroprolactinoma) (Fig. 3b) and confirmation of suspected intra/parasellar calcification [e.g. calcified PA (with thyrotropinoma being the classic example) or craniopharyngioma] (Fig. 3c). CT is also used in conjunction with MRI to facilitate radiotherapy planning and may reveal previously unsuspected tumour invasion of bony structures(18,19).

Insert Figure 3 here

Functional Pituitary Imaging

Despite recent advances in cross-sectional imaging, there remain several situations in which clinical decision-making is limited by indeterminate MRI and/or CT findings, including:

(i) small PA that cannot be readily visualised even using a combination of sequences (e.g. corticotroph adenomas may evade detection in 30-40% of patients with Cushing disease(20); similarly, thyrotroph and lactotroph tumours are not always easily localised)
(ii) following primary intervention (surgery, radiotherapy or medical therapy) when post-treatment change may be difficult to distinguish from residual functioning tumour
(iii) in the presence of a confounding pituitary incidentaloma

Functional imaging represents an alternative and complementary approach to traditional anatomical imaging and has found widespread use in many endocrine disorders [e.g. technetium-99m-pertechnetate and technetium-99m-sestamibi scintigraphy in hyperthyroidism and hyperparathyroidism respectively; ^{123}I-metaiodobenzylguanidine (^{123}I-MIBG) scintigraphy for detection of phaeochromocytoma/paraganglioma]. However, while scintigraphy remains a useful clinical technique, especially when combined with single photon emission computed tomography (SPECT) for image acquisition, its application in other fields of endocrinology has been limited by its modest sensitivity for detecting small lesions.

Positron emission tomography (PET) offers a solution to this problem and can be combined with CT (PET/CT) or MRI (PET/MR) to allow detection of even subcentimetre lesions. The development of PET ligands targeting different cellular processes (e.g. glucose or amino acid uptake, receptor or intracellular enzyme expression) has opened up new opportunities for the application of PET in endocrine disorders. The potential superiority of PET over conventional scintigraphy is exemplified by the comparison of ^{111}Indium-pentetreotide scintigraphy (± SPECT) ('octreoscan') and ^{68}Gallium-DOTATATE PET/CT for the

investigation of neuroendocrine tumours (NET), where the latter often detects lesions not seen on a conventional octreoscan(21).

To date, functional imaging has found limited use in the routine management of pituitary adenomas, although several groups have explored various modalities including somatostatin receptor scintigraphy (SRS) or PET, ^{18}F-fluorodeoxyglucose (18F-FDG)-PET and ^{11}C-methionine(^{11}C-Met)-PET.

Somatostatin Receptor Scintigraphy and PET

Somatostatin receptors (SSTRs) are expressed in normal human pituitary tissue and, to varying degrees, in different subtypes of pituitary adenoma. For example, somatostatin receptor subtype 2 (SSTR2) is detectable in most somatotroph adenomas, whereas SSTR5 expression is more variable(22). In contrast, corticotroph adenomas express higher levels of SSTR3 and SSTR5, but have also recently been confirmed to express SSTR2A(23). The use of Somatostatin Receptor Scintigraphy (e.g. ^{111}Indium-pentetreotide) in the investigation and management of PA is therefore confounded by several factors: background uptake by normal pituitary tissue; dependence on SSTR subtype expression of the tumour; and limited spatial resolution and sensitivity of scintigraphy, even when combined with SPECT. ^{68}Ga-DOTATATE PET has the potential to address the latter, but it has yet to find clear utility in the management of PA, although preliminary data suggests that combination with ^{18}F-FDG PET may allow distinction of normal gland and adenoma in some cases of primary and recurrent disease(24,25).

^{18}F-FDG PET

The literature contains numerous case reports of incidentally-detected ^{18}F-FDG uptake by pituitary adenoma(26–29). In contrast, in a large retrospective analysis of incidental pituitary uptake in >40,000 patients who had undergone whole body FDG PET/CT, the overall incidence was just 0.073%(30). Together these findings (demonstrable uptake by PA with a

negligible false positive rate) suggest a possible role for ^{18}F-FDG PET in pituitary imaging. Indeed, the potential utility of ^{18}F-FDG PET has been explored in various subtypes of PA(24,25). but has been most extensively studied in the context of corticotroph tumours, which often evade detection on MRI. However, findings have been largely disappointing. In a prospective study of ten consecutive patients with subsequently confirmed CD, high resolution ^{18}F-FDG PET (^{18}F-FDG hrPET) was performed together with SE and SPGR MRI(31). ^{18}F-FDG hrPET revealed increased tracer uptake in four patients, two of whom had no demonstrable lesion on SE MRI. However, SPGR proved more sensitive than ^{18}F-FDG hrPET, identifying a pituitary adenoma in seven cases and, importantly, no adenomas were detected by ^{18}F-FDG hrPET that were not visualised on SPGR MRI. A comparable detection rate (58%) was reported by Alzahrani and colleagues in their retrospective study of 12 patients who underwent conventional ^{18}F-FDG PET/CT(32). Accordingly, ^{18}F-FDG PET has yet to find a place in the routine management of PA.

^{11}C-methionine PET

Several groups have demonstrated the potential utility of ^{11}C-methionine PET/CT (Met-PET/CT) in different pituitary tumour subtypes, both for the localisation of *de novo* tumours, especially microadenomas, and also for the identification of persistent or recurrent disease(18,33–36). However, a key limitation of Met-PET/CT is the relative lack of anatomical detail provided by CT when compared with MRI. This has led us and other workers to explore the possibility of fusing functional images derived from PET-CT with cross-sectional images obtained during volumetric MRI (e.g. FSPGR MRI)(35–38). In this way, the precise site(s) of ^{11}C-methionine uptake can be delineated through coregistration of PET/CT and MRI images. With the advent of PET/MR this process will become even easier and more convenient, as has been demonstrated with other tracers(25).

However, several important considerations must be taken in to account when developing a specialist pituitary imaging service using ^{11}C-methionine PET.

Patient selection and preparation

Careful case selection is important. The majority of patients with PA do not require molecular imaging. However, the ability to correlate structure with function is potentially useful when either a small *de novo* functioning tumour (e.g. in Cushing disease, thyrotropinoma, prolactinoma or, less commonly, acromegaly), or residual/recurrent functioning PA (e.g. acromegaly) cannot be reliably identified on good quality MRI, and when definitive treatment (TSS or SRS) would otherwise be considered. As molecular imaging with ^{11}C-methionine depends on the presence of functioning adenoma tissue, it is important to ensure adequate washout of agents that might otherwise suppress hormone production by the tumour [e.g. SSA or dopamine agonist (DA) therapy in acromegaly], and to confirm active disease prior to imaging. We recommend discontinuation of short-acting SSA therapy (i.e. octreotide) and DA at least one month prior to scanning. For depot SSA (e.g. Sandostatin LAR® or Lanreotide Autogel®) a longer washout period is required (typically 3 months). Patients should be instructed to fast for at least 4 hours before the scan. On the day, a further assessment of disease activity [paired random GH and IGF-1 in acromegaly; paired 9am adrenocorticotrophic hormone (ACTH) and cortisol followed by late night salivary cortisol in Cushing syndrome; paired free thyroxine and TSH in thyrotropinoma; prolactin in prolactinoma], together with assessment of remaining pituitary function, should be undertaken.

Tracer production

Carbon-11 (^{11}C) has a half-life of just 20 minutes and is synthesised using a particle accelerator (Cyclotron). Following production, several quality control steps (identification, purity, stability, half-life confirmation, pH detection and substance sterility) must be completed

before the tracer can be administered(39). The short half-life therefore limits its use to centres with an in-house cyclotron. Typically, between 100 and 400 MBq is administered intravenously.

PET acquisition

Uptake time is typically standardised (e.g. 20 min) following tracer injection. Acquisition of low dose CT images allows for attenuation correction (AC) of the PET dataset. A similar approach is required for hybrid PET/MR systems(40–43).

PET/CT-MRI coregistration

^{11}C-methionine PET/CT coregistration to independently acquired MRI (Met-PET-MRI^{CR}) can be performed using commercially available image fusion software. Amongst the most commonly used are automated (e.g. GE Xeleris®) and manual (e.g. MedCom Prosoma® and Slicer®) systems(44–46). Volumetric (1mm thickness) MRI facilitates coregistration.

^{11}C-methionine PET/CT-MRI findings in different PA subtypes

Prolactinoma

Lactotroph PA generally demonstrate avid ^{11}C-methionine uptake (up to 9 times background brain uptake). In patients with hyperprolactinaemia for whom medical therapy with DA is not tolerated or advised, and in whom pituitary MRI is indeterminate, Met-PET-MRI^{CR} can facilitate localisation of the tumour to guide selective TSS (Fig. 4). Similarly, in drug resistant macroprolactinomas the site(s) of residual disease can be readily localized to help the pituitary multidisciplinary team decide whether surgery or RT is appropriate (Bashari, Koulouri and Gurnell, unpublished data).

Insert Figure 4 here

Acromegaly

Similar to lactotroph tumours, somatotropinomas avidly take up ^{11}C-methionine and Met-PET-MRI^{CR} can help distinguish metabolically active residual/recurrent PA from scar tissue(36). As indicated above, certain types of medical therapy (e.g. SSA, DA) can diminish tracer uptake and appropriate washout should be completed before imaging is performed(36).

Insert Figure 5 here

Cushing disease

^{11}C-methionine uptake by corticotroph adenomas is typically less than is seen in other pituitary tumour subtypes. Possible reasons for this include the relatively low representation of corticotrophs amongst anterior pituitary cells (10-20%); their localization in the centre of the gland (leading to additional challenges due to tumoral tracer uptake merging with that of the normal gland); in addition, the periodic/cyclical nature of ACTH production in some corticotroph tumours may result in low uptake if the patient is scanned when the tumour is relatively quiescent (hence the need to confirm active disease at the time of imaging). Accordingly, success rates for localizing *de novo* or recurrent corticotroph tumours are of the order of ~70% (Fig. 6).

Insert Figure 6 here

TSH-secreting PA (thyrotropinoma)

The majority of thyrotroph tumours demonstrate avid uptake of ^{11}C-methionine (Fig. 7). We have also shown that this uptake can be suppressed by SSA therapy, thus providing an 'endocrine switch' which can offer added reassurance when MR findings are unconvincing for the presence of an adenoma(37).

Insert Figure 7 here

Clinically non-functioning pituitary adenoma / gonadotropinoma

Clinically non-functioning PAs (NFPA) and functioning gonadotropinomas also demonstrate significant ^{11}C-methionine uptake which can therefore be used as a biomarker of residual/recurrent disease (Fig. 8).

Insert Figure 8 here

Reassuringly, ^{11}C-methionine uptake by cystic pituitary lesions within the sella is typically low/absent when compared with the normal background pituitary tissue or a PA (Fig. 9).

Insert Figure 9 here

Summary

In the majority of cases when pituitary imaging is indicated, good quality T1 (± contrast enhancement) and T2 weighted sequences will provide sufficient information to allow effective clinical decision making. For those patients in whom MRI findings are inconclusive, consideration should be given to the use of other MR sequences, but these should only be requested following discussion with the pituitary multidisciplinary team (MDT). When MRI is not possible or tolerated, thin slice pituitary CT is a reasonable alternative, while in other situations it can augment the findings from MRI (e.g. when bony invasion/destruction is suspected). Although functional imaging with molecular PET tracers (e.g. ^{11}C-methionine) is unlikely to find widespread usage, emerging evidence suggests that in a subgroup of patients it may play an important role in facilitating (further) definitive intervention (e.g. TSS or RT), thereby sparing patients and healthcare systems the need for long-term, often expensive, medical therapy. The establishment of a small number of centres with expertise in molecular pituitary imaging may sit comfortably with the recently proposed model for Pituitary Tumor Centres of Excellence (PTCOE)(47).

Practice Points

- All clinicians involved in the management of pituitary patients should have a good understanding of the MR sequences that are routinely used for pituitary imaging in their centre and when to consider alternative MR protocols.
- The decision to request gadolinium-enhanced MR sequences (e.g. T1 weighted with contrast) should include careful consideration of recent concerns raised regarding gadolinium deposition with GBCAs – if in doubt then discuss with the pituitary MDT and consider the use of alternative sequences (e.g. T2 weighted).
- Pituitary CT is indicated when MRI is not possible or tolerated, and when there is concern regarding bone invasion/destruction or intratumoral calcification.
- Functional imaging with the molecular tracer ^{11}C-methionine (Met-PET-MRI^{CR}) can help

identify *de novo* or residual/recurrent PA in all tumour subtypes when MRI findings are inconclusive.

Research Agenda

- It remains unclear whether the advent of MR scanners with increased magnetic field strength (e.g. 7T) will bring added benefits that outweigh the potential disadvantages of identifying a greater proportion of confounding incidental pituitary lesions. Further studies are awaited.
- Although several MRI protocols that find routine use in other clinical settings (e.g. DWI, Elastography) have been applied to pituitary imaging with promising results, further studies are needed to determine whether these should be adopted in to routine clinical practice.
- Functional imaging with the molecular tracer ^{11}C-methionine (Met-PET-MRI^{CR} or Met-PET/MRI) shows significant promise for producing a step change in the management of a subgroup of patients with PA. However, challenges remain when handling the raw datasets and collaborative studies drawing on the expertise of colleagues in the applied sciences (mathematics, physics) will likely be required to take image analysis to the next level.

Disclosures

None of the authors have anything to disclose.

Acknowledgements

This work was supported by the UK NIHR Cambridge Biomedical Research Centre and by the Evelyn Trust.

Author ORCID IDs

Waiel Bashari	0000-0002-2204-9169
Russell Senanayake	0000-0002-4141-1709
Antia Fernandez-Pombo	0000-0002-1268-7538
Olympia Koulori	
Andrew Powlson	
Daniel Scoffings	
Iosif Mendichovszky	0000-0002-3777-2827
Heok Cheow	
Mark Gurnell	0000-0001-5745-6832

References:

1. Vandeva S, Jaffrain-Rea M-L, Daly AF, Tichomirowa M, Zacharieva S, Beckers A. The genetics of pituitary adenomas. Best Pract Res Clin Endocrinol Metab [Internet]. 2010 Jun [cited 2019 Apr 23];24(3):461–76. Available from: http://www.ncbi.nlm.nih.gov/pubmed/20833337
2. Ezzat S, Asa SL, Couldwell WT, Barr CE, Dodge WE, Vance ML, et al. The prevalence of pituitary adenomas. Cancer [Internet]. 2004 Aug 1 [cited 2019 Apr 23];101(3):613–9. Available from: http://www.ncbi.nlm.nih.gov/pubmed/15274075
3. Sherlock M, Woods C, Sheppard MC. Medical therapy in acromegaly. Nat Rev Endocrinol [Internet]. 2011 May 29 [cited 2019 Apr 23];7(5):291–300. Available from: http://www.ncbi.nlm.nih.gov/pubmed/21448141
4. Elster AD. Modern imaging of the pituitary. Radiology [Internet]. 1993 Apr [cited 2019 Apr 23];187(1):1–14. Available from: http://www.ncbi.nlm.nih.gov/pubmed/8451394
5. Bonneville J-F, Bonneville F, Cattin F. Magnetic resonance imaging of pituitary adenomas. Eur Radiol [Internet]. 2005 Mar 31 [cited 2019 Apr 23];15(3):543–8. Available from: http://www.ncbi.nlm.nih.gov/pubmed/15627195
6.* Bonneville J-F. Magnetic Resonance Imaging of Pituitary Tumors. Front Horm Res [Internet]. 2016;45:97–120. Available from: http://www.ncbi.nlm.nih.gov/pubmed/27003878
7. Nachtigall LB, Karavitaki N, Kiseljak-Vassiliades K, Ghalib L, Fukuoka H, Syro L V., et al. Physicians' awareness of gadolinium retention and MRI timing practices in the longitudinal management of pituitary tumors: a "Pituitary Society" survey. Pituitary [Internet]. 2019 Feb 19 [cited 2019 Apr 23];22(1):37–45. Available from: http://www.ncbi.nlm.nih.gov/pubmed/30456434
8.* Bonneville J-F. A plea for the T2W MR sequence for pituitary imaging. Pituitary [Internet]. 2019 Apr 28 [cited 2019 Apr 23];22(2):195–7. Available from: http://link.springer.com/10.1007/s11102-018-0928-9
9. Chowdhury IN, Sinaii N, Oldfield EH, Patronas N, Nieman LK. A change in pituitary magnetic resonance imaging protocol detects ACTH-secreting tumours in patients with previously negative results. Clin Endocrinol (Oxf). 2010;72(4):502–6.
10. Wolfsberger S, Ba-Ssalamah A, Pinker K, Mlynárik V, Czech T, Knosp E, et al. Application of three-tesla magnetic resonance imaging for diagnosis and surgery of sellar lesions. J Neurosurg [Internet]. 2004 Feb [cited 2019 Apr 23];100(2):278–86. Available from: http://www.ncbi.nlm.nih.gov/pubmed/15086236
11. de Rotte AAJ, van der Kolk AG, Rutgers D, Zelissen PMJ, Visser F, Luijten PR, et al. Feasibility of high-resolution pituitary MRI at 7.0 tesla. Eur Radiol [Internet]. 2014 Aug 29 [cited 2019 Apr 23];24(8):2005–11. Available from: http://www.ncbi.nlm.nih.gov/pubmed/24871334
12. Rutland JW, Padormo F, Yim CK, Yao A, Arrighi-Allisan A, Huang K-H, et al. Quantitative assessment of secondary white matter injury in the visual pathway by pituitary adenomas: a multimodal study at 7-Tesla MRI. J Neurosurg [Internet]. 2019 Jan 18 [cited 2019 Apr 23];1–10. Available from: http://www.ncbi.nlm.nih.gov/pubmed/30660127
13. Erickson D, Erickson B, Watson R, Patton A, Atkinson J, Meyer F, et al. 3 Tesla magnetic resonance imaging with and without corticotropin releasing hormone stimulation for the detection of microadenomas in Cushing's syndrome. Clin Endocrinol (Oxf). 2010;72(6):793–9.
14.* Knosp E, Steiner E, Kitz K, Matula C. Pituitary adenomas with invasion of the cavernous sinus space: a magnetic resonance imaging classification compared with

surgical findings. Neurosurgery [Internet]. 1993 Oct [cited 2019 Apr 23];33(4):610–7; discussion 617-8. Available from: http://www.ncbi.nlm.nih.gov/pubmed/8232800
15.* Micko ASG, Wöhrer A, Wolfsberger S, Knosp E. Invasion of the cavernous sinus space in pituitary adenomas: endoscopic verification and its correlation with an MRI-based classification. J Neurosurg [Internet]. 2015 Apr [cited 2019 Apr 23];122(4):803–11. Available from: http://www.ncbi.nlm.nih.gov/pubmed/25658782
16.* Grober Y, Grober H, Wintermark M, Jane JA, Oldfield EH. Comparison of MRI techniques for detecting microadenomas in Cushing's disease. J Neurosurg. 2018;128(4):1051–7.
17. Kinoshita M, Tanaka H, Arita H, Goto Y, Oshino S, Watanabe Y, et al. Pituitary-Targeted Dynamic Contrast-Enhanced Multisection CT for Detecting MR Imaging–Occult Functional Pituitary Microadenoma. Am J Neuroradiol [Internet]. 2015 May [cited 2019 Apr 23];36(5):904–8. Available from: http://www.ncbi.nlm.nih.gov/pubmed/25593201
18. Taku N, Koulouri O, Scoffings D, Gurnell M, Burnet N. The use of 11carbon methionine positron emission tomography (PET) imaging to enhance radiotherapy planning in the treatment of a giant, invasive pituitary adenoma. BJR case reports [Internet]. 2017 [cited 2019 Apr 23];3(2):20160098. Available from: http://www.ncbi.nlm.nih.gov/pubmed/30363212
19. Minniti G, Osti MF, Niyazi M. Target delineation and optimal radiosurgical dose for pituitary tumors. Radiat Oncol [Internet]. 2016 Dec 11 [cited 2019 Apr 23];11(1):135. Available from: http://www.ncbi.nlm.nih.gov/pubmed/27729088
20. Patronas N, Bulakbasi N, Stratakis CA, Lafferty A, Oldfield EH, Doppman J, et al. Spoiled Gradient Recalled Acquisition in the Steady State Technique Is Superior to Conventional Postcontrast Spin Echo Technique for Magnetic Resonance Imaging Detection of Adrenocorticotropin-Secreting Pituitary Tumors. J Clin Endocrinol Metab [Internet]. 2003 Apr [cited 2019 Apr 23];88(4):1565–9. Available from: http://www.ncbi.nlm.nih.gov/pubmed/12679440
21. Challis BG, Powlson AS, Casey RT, Pearson C, Lam BY, Ma M, et al. Adult-onset hyperinsulinaemic hypoglycaemia in clinical practice: diagnosis, aetiology and management. Endocr Connect [Internet]. 2017 Oct [cited 2019 Apr 23];6(7):540–8. Available from: http://www.ncbi.nlm.nih.gov/pubmed/28784625
22. Nielsen S, Mellemkjær S, Rasmussen LM, Ledet T, Olsen N, Bojsen-Møller M, et al. Expression of somatostatin receptors on human pituitary adenomas in vivo and ex vivo. J Endocrinol Invest [Internet]. 2001 Jun 29 [cited 2019 Apr 23];24(6):430–7. Available from: http://www.ncbi.nlm.nih.gov/pubmed/11434667
23. Behling F, Honegger J, Skardelly M, Gepfner-Tuma I, Tabatabai G, Tatagiba M, et al. High Expression of Somatostatin Receptors 2A, 3, and 5 in Corticotroph Pituitary Adenoma. Int J Endocrinol [Internet]. 2018 Dec 9 [cited 2019 Apr 23];2018:1–12. Available from: https://www.hindawi.com/journals/ije/2018/1763735/
24.* Zhao X, Xiao J, Xing B, Wang R, Zhu Z, Li F. Comparison of 68Ga DOTATATE to 18F-FDG Uptake Is Useful in the Differentiation of Residual or Recurrent Pituitary Adenoma From the Remaining Pituitary Tissue After Transsphenoidal Adenomectomy. Clin Nucl Med [Internet]. 2014 Jul [cited 2019 Apr 23];39(7):605–8. Available from: http://content.wkhealth.com/linkback/openurl?sid=WKPTLP:landingpage&an=00003072-201407000-00003
25. Wang H, Hou B, Lu L, Feng M, Zang J, Yao S, et al. PET/MR imaging in the diagnosis of hormone-producing pituitary micro-adenoma: a prospective pilot study. J Nucl Med. 2017;

26. CAMPEAU RJ, DAVID O, DOWLING AM. Pituitary Adenoma Detected on FDG Positron Emission Tomography in a Patient with Mucosa-Associated Lymphoid Tissue Lymphoma. Clin Nucl Med [Internet]. 2003 Apr [cited 2019 Apr 23];28(4):296–8. Available from: https://insights.ovid.com/crossref?an=00003072-200304000-00005
27. Ryu SI, Tafti BA, Skirboll SL. Pituitary Adenomas Can Appear as Hypermetabolic Lesions in 18F-FDG PET Imaging. J Neuroimaging [Internet]. 2010 Oct [cited 2019 Apr 23];20(4):393–6. Available from: http://www.ncbi.nlm.nih.gov/pubmed/19453834
28. Maffei P, Marzola MC, Musto A, Dassie F, Grassetto G, De Carlo E, et al. A Very Rare Case of Nonfunctioning Pituitary Adenoma Incidentally Disclosed at 18F-FDG PET/CT. Clin Nucl Med [Internet]. 2012 May [cited 2019 Apr 23];37(5):e100–1. Available from: https://insights.ovid.com/crossref?an=00003072-201205000-00028
29. Joshi P, Lele V, Gandhi R. Incidental detection of clinically occult follicle stimulating hormone secreting pituitary adenoma on whole body 18-Fluorodeoxyglucose positron emission tomography-computed tomography. Indian J Nucl Med [Internet]. 2011 Jan [cited 2019 Apr 23];26(1):34–5. Available from: http://www.ncbi.nlm.nih.gov/pubmed/21969778
30. Jeong SY, Lee S-W, Lee HJ, Kang S, Seo J-H, Chun KA, et al. Incidental pituitary uptake on whole-body 18F-FDG PET/CT: a multicentre study. Eur J Nucl Med Mol Imaging [Internet]. 2010 Dec 27 [cited 2019 Apr 23];37(12):2334–43. Available from: http://www.ncbi.nlm.nih.gov/pubmed/20661556
31. Chittiboina P, Montgomery BK, Millo C, Herscovitch P, Lonser RR. High-resolution(18)F-fluorodeoxyglucose positron emission tomography and magnetic resonance imaging for pituitary adenoma detection in Cushing disease. J Neurosurg [Internet]. 2015 Apr [cited 2019 Apr 23];122(4):791–7. Available from: http://www.ncbi.nlm.nih.gov/pubmed/25479121
32. Alzahrani AS, Farhat R, Al-Arifi A, Al-Kahtani N, Kanaan I, Abouzied M. The diagnostic value of fused positron emission tomography/computed tomography in the localization of adrenocorticotropin-secreting pituitary adenoma in Cushing's disease. Pituitary [Internet]. 2009 Dec 22 [cited 2019 Apr 23];12(4):309–14. Available from: http://www.ncbi.nlm.nih.gov/pubmed/19387839
33. Feng Z, He D, Mao Z, Wang Z, Zhu Y, Zhang X, et al. Utility of 11C-Methionine and 18F-FDG PET/CT in Patients With Functioning Pituitary Adenomas. Clin Nucl Med [Internet]. 2016 Mar [cited 2019 Apr 23];41(3):e130–4. Available from: http://www.ncbi.nlm.nih.gov/pubmed/26646998
34. Muhr C. Positron Emission Tomography in Acromegaly and Other Pituitary Adenoma Patients. Neuroendocrinology [Internet]. 2006 [cited 2019 Apr 23];83(3–4):205–10. Available from: https://www.karger.com/Article/FullText/95529
35.* Koulouri O, Steuwe A, Gillett D, Hoole AC, Powlson AS, Donnelly NA, et al. A role for 11C-methionine PET imaging in ACTH-dependent Cushing's syndrome. Eur J Endocrinol [Internet]. 2015 Oct;173(4):M107–20. Available from: https://eje.bioscientifica.com/view/journals/eje/173/4/M107.xml
36.* Koulouri O, Kandasamy N, Hoole AC, Gillett D, Heard S, Powlson AS, et al. Successful treatment of residual pituitary adenoma in persistent acromegaly following localisation by 11C-methionine PET co-registered with MRI. Eur J Endocrinol. 2016;
37.* Koulouri O, Hoole AC, English P, Allinson K, Antoun N, Cheow H, et al. Localisation of an occult thyrotropinoma with 11C-methionine PET-CT before and after somatostatin analogue therapy. Vol. 4, The Lancet Diabetes and Endocrinology. 2016. p. 1050.
38. Ikeda H, Abe T, Watanabe K. Usefulness of composite methionine–positron emission tomography/3.0-tesla magnetic resonance imaging to detect the localization and extent

of early-stage Cushing adenoma. J Neurosurg [Internet]. 2010 Apr [cited 2019 Apr 23];112(4):750–5. Available from: http://www.ncbi.nlm.nih.gov/pubmed/19698042
39. Kilian K, Pękal A, Juszczyk J. Synthesis of 11C-methionine through gas phase iodination using Synthra MeIPlus synthesis module. Nukleonika [Internet]. 2016 Mar 1 [cited 2019 Apr 23];61(1):29–33. Available from: http://content.sciendo.com/view/journals/nuka/61/1/article-p29.xml
40. Delso G, Gillett D, Bashari W, Matys T, Mendichovszky I, Gurnell M. Clinical evaluation of ^{11}C-Met-avid pituitary lesions using a ZTE-based AC method. IEEE Trans Radiat Plasma Med Sci [Internet]. 2018 [cited 2019 Apr 23];1–1. Available from: https://ieeexplore.ieee.org/document/8576584/
41. Vandenberghe S, Marsden PK. PET-MRI: a review of challenges and solutions in the development of integrated multimodality imaging. Phys Med Biol [Internet]. 2015 Feb 21 [cited 2019 Apr 23];60(4):R115–54. Available from: http://www.ncbi.nlm.nih.gov/pubmed/25650582
42. Wagenknecht G, Kaiser H-J, Mottaghy FM, Herzog H. MRI for attenuation correction in PET: methods and challenges. Magn Reson Mater Physics, Biol Med [Internet]. 2013 Feb 21 [cited 2019 Apr 23];26(1):99–113. Available from: http://link.springer.com/10.1007/s10334-012-0353-4
43. Hofmann M, Steinke F, Scheel V, Charpiat G, Farquhar J, Aschoff P, et al. MRI-Based Attenuation Correction for PET/MRI: A Novel Approach Combining Pattern Recognition and Atlas Registration. J Nucl Med [Internet]. 2008 Oct 16 [cited 2019 Apr 23];49(11):1875–83. Available from: http://www.ncbi.nlm.nih.gov/pubmed/18927326
44. Pooler AM, Mayles HM, Naismith OF, Sage JP, Dearnaley DP. Evaluation of margining algorithms in commercial treatment planning systems. Radiother Oncol [Internet]. 2008 Jan [cited 2019 Apr 23];86(1):43–7. Available from: http://www.ncbi.nlm.nih.gov/pubmed/18054103
45. Fedorov A, Beichel R, Kalpathy-Cramer J, Finet J, Fillion-Robin J-C, Pujol S, et al. 3D Slicer as an image computing platform for the Quantitative Imaging Network. Magn Reson Imaging [Internet]. 2012 Nov [cited 2019 Apr 23];30(9):1323–41. Available from: http://www.ncbi.nlm.nih.gov/pubmed/22770690
46. Velazquez ER, Parmar C, Jermoumi M, Mak RH, van Baardwijk A, Fennessy FM, et al. Volumetric CT-based segmentation of NSCLC using 3D-Slicer. Sci Rep [Internet]. 2013 Dec 18 [cited 2019 Apr 23];3(1):3529. Available from: http://www.ncbi.nlm.nih.gov/pubmed/24346241
47. Casanueva FF, Barkan AL, Buchfelder M, Klibanski A, Laws ER, Loeffler JS, et al. Criteria for the definition of Pituitary Tumor Centers of Excellence (PTCOE): A Pituitary Society Statement. Pituitary. 2017;20(5):489–98.
48. Cazabat L, Dupuy M, Boulin A, Bernier M, Baussart B, Foubert L, et al. Silent, but not unseen: multimicrocystic aspect on T2-weighted MRI in silent corticotroph adenomas. Clin Endocrinol (Oxf) [Internet]. 2014 Oct [cited 2019 Apr 23];81(4):566–72. Available from: http://www.ncbi.nlm.nih.gov/pubmed/24601912
49. Potorac I, Beckers A, Bonneville J-F. T2-weighted MRI signal intensity as a predictor of hormonal and tumoral responses to somatostatin receptor ligands in acromegaly: a perspective. Pituitary [Internet]. 2017 Feb 14 [cited 2019 Apr 23];20(1):116–20. Available from: http://www.ncbi.nlm.nih.gov/pubmed/28197813
50.* Heck A, Emblem KE, Casar-Borota O, Bollerslev J, Ringstad G. Quantitative analyses of T2-weighted MRI as a potential marker for response to somatostatin analogs in newly diagnosed acromegaly. Endocrine [Internet]. 2016 May 16 [cited 2019 Apr 23];52(2):333–43. Available from: http://www.ncbi.nlm.nih.gov/pubmed/26475495

51. Rogg JM, Tung GA, Anderson G, Cortez S. Pituitary apoplexy: early detection with diffusion-weighted MR imaging. AJNR Am J Neuroradiol [Internet]. 2002 Aug [cited 2019 Apr 23];23(7):1240–5. Available from: http://www.ncbi.nlm.nih.gov/pubmed/12169486
52. Kunii N, Abe T, Kawamo M, Tanioka D, Izumiyama H, Moritani T. Rathke's cleft cysts: differentiation from other cystic lesions in the pituitary fossa by use of single-shot fast spin-echo diffusion-weighted MR imaging. Acta Neurochir (Wien) [Internet]. 2007 Aug 9 [cited 2019 Apr 23];149(8):759–69. Available from: http://www.ncbi.nlm.nih.gov/pubmed/17594050
53. Pierallini A, Caramia F, Falcone C, Tinelli E, Paonessa A, Ciddio AB, et al. Pituitary Macroadenomas: Preoperative Evaluation of Consistency with Diffusion-weighted MR Imaging—Initial Experience. Radiology [Internet]. 2006 Apr [cited 2019 Apr 23];239(1):223–31. Available from: http://www.ncbi.nlm.nih.gov/pubmed/16452397
54. Wang M, Liu H, Wei X, Liu C, Liang T, Zhang X, et al. Application of Reduced-FOV Diffusion-Weighted Imaging in Evaluation of Normal Pituitary Glands and Pituitary Macroadenomas. AJNR Am J Neuroradiol [Internet]. 2018 Aug 1 [cited 2019 Apr 23];39(8):1499–504. Available from: http://www.ncbi.nlm.nih.gov/pubmed/30026383
55. Yiping L, Ji X, Daoying G, Bo Y. Prediction of the consistency of pituitary adenoma: A comparative study on diffusion-weighted imaging and pathological results. J Neuroradiol [Internet]. 2016 Jun [cited 2019 Apr 23];43(3):186–94. Available from: http://www.ncbi.nlm.nih.gov/pubmed/26585529
56. Mahmoud OM, Tominaga A, Amatya VJ, Ohtaki M, Sugiyama K, Sakoguchi T, et al. Role of PROPELLER diffusion-weighted imaging and apparent diffusion coefficient in the evaluation of pituitary adenomas. Eur J Radiol [Internet]. 2011 Nov [cited 2019 Apr 23];80(2):412–7. Available from: http://www.ncbi.nlm.nih.gov/pubmed/20580505
57. Sanei Taheri M, Kimia F, Mehrnahad M, Saligheh Rad H, Haghighatkhah H, Moradi A, et al. Accuracy of diffusion-weighted imaging-magnetic resonance in differentiating functional from non-functional pituitary macro-adenoma and classification of tumor consistency. Neuroradiol J [Internet]. 2019 Apr 3 [cited 2019 Apr 23];32(2):74–85. Available from: http://journals.sagepub.com/doi/10.1177/1971400918809825
58. Suzuki C, Maeda M, Hori K, Kozuka Y, Sakuma H, Taki W, et al. Apparent diffusion coefficient of pituitary macroadenoma evaluated with line-scan diffusion-weighted imaging. J Neuroradiol [Internet]. 2007 Oct [cited 2019 Apr 23];34(4):228–35. Available from: http://www.ncbi.nlm.nih.gov/pubmed/17719632
59. Yu CS, Li KC, Xuan Y, Ji XM, Qin W. Diffusion tensor tractography in patients with cerebral tumors: A helpful technique for neurosurgical planning and postoperative assessment. Eur J Radiol [Internet]. 2005 Nov [cited 2019 Apr 23];56(2):197–204. Available from: http://www.ncbi.nlm.nih.gov/pubmed/15916876
60. Salmela MB, Cauley KA, Nickerson JP, Koski CJ, Filippi CG. Magnetic resonance diffusion tensor imaging (MRDTI) and tractography in children with septo-optic dysplasia. Pediatr Radiol [Internet]. 2010 May 9 [cited 2019 Apr 23];40(5):708–13. Available from: http://link.springer.com/10.1007/s00247-009-1478-0
61. Anik I, Anik Y, Cabuk B, Caklili M, Pirhan D, Ozturk O, et al. Visual Outcome of an Endoscopic Endonasal Transsphenoidal Approach in Pituitary Macroadenomas: Quantitative Assessment with Diffusion Tensor Imaging Early and Long-Term Results. World Neurosurg [Internet]. 2018 Apr [cited 2019 Apr 23];112:e691–701. Available from: http://www.ncbi.nlm.nih.gov/pubmed/29408649
62. Ma Z, He W, Zhao Y, Yuan J, Zhang Q, Wu Y, et al. Predictive value of PWI for blood supply and T1-spin echo MRI for consistency of pituitary adenoma.

Neuroradiology [Internet]. 2016 Jan 16 [cited 2019 Apr 23];58(1):51–7. Available from: http://www.ncbi.nlm.nih.gov/pubmed/26376802
63. Bladowska J, Zimny A, Guziński M, Hałoń A, Tabakow P, Czyż M, et al. Usefulness of perfusion weighted magnetic resonance imaging with signal-intensity curves analysis in the differential diagnosis of sellar and parasellar tumors: Preliminary report. Eur J Radiol [Internet]. 2013 Aug [cited 2019 Apr 23];82(8):1292–8. Available from: http://www.ncbi.nlm.nih.gov/pubmed/23466030
64. Hakyemez B, Yildirim N, Erdoðan C, Kocaeli H, Korfali E, Parlak M. Meningiomas with conventional MRI findings resembling intraaxial tumors: can perfusion-weighted MRI be helpful in differentiation? Neuroradiology [Internet]. 2006 Oct 2 [cited 2019 Apr 23];48(10):695–702. Available from: http://www.ncbi.nlm.nih.gov/pubmed/16896907
65. Manara R, Maffei P, Citton V, Rizzati S, Bommarito G, Ermani M, et al. Increased Rate of Intracranial Saccular Aneurysms in Acromegaly: An MR Angiography Study and Review of the Literature. J Clin Endocrinol Metab [Internet]. 2011 May 1 [cited 2019 Apr 23];96(5):1292–300. Available from: https://academic.oup.com/jcem/article-lookup/doi/10.1210/jc.2010-2721
66. Linn J, Peters F, Lummel N, Schankin C, Rachinger W, Brueckmann H, et al. Detailed imaging of the normal anatomy and pathologic conditions of the cavernous region at 3 Tesla using a contrast-enhanced MR angiography. Neuroradiology [Internet]. 2011 Dec 27 [cited 2019 Apr 23];53(12):947–54. Available from: http://www.ncbi.nlm.nih.gov/pubmed/21271242
67. Hughes JD, Fattahi N, Van Gompel J, Arani A, Ehman R, Huston J. Magnetic resonance elastography detects tumoral consistency in pituitary macroadenomas. Pituitary [Internet]. 2016 Jun 18 [cited 2019 Apr 23];19(3):286–92. Available from: http://www.ncbi.nlm.nih.gov/pubmed/26782836
68. Pînzariu O, Georgescu B, Georgescu CE. Metabolomics—A Promising Approach to Pituitary Adenomas. Front Endocrinol (Lausanne) [Internet]. 2019 Jan 17 [cited 2019 Apr 23];9:814. Available from: https://www.frontiersin.org/article/10.3389/fendo.2018.00814/full
69. Chernov MF, Kawamata T, Amano K, Ono Y, Suzuki T, Nakamura R, et al. Possible role of single-voxel 1H-MRS in differential diagnosis of suprasellar tumors. J Neurooncol [Internet]. 2009 Jan 30 [cited 2019 Apr 23];91(2):191–8. Available from: http://www.ncbi.nlm.nih.gov/pubmed/18825316
70. Sutton LN, Wang ZJ, Wehrli SL, Marwaha S, Molloy P, Phillips PC, et al. Proton spectroscopy of suprasellar tumors in pediatric patients. Neurosurgery [Internet]. 1997 Aug [cited 2019 Apr 23];41(2):388–94; discussion 394-5. Available from: http://www.ncbi.nlm.nih.gov/pubmed/9257306
71. Hu J, Yan J, Zheng X, Zhang Y, Ran Q, Tang X, et al. Magnetic resonance spectroscopy may serve as a presurgical predictor of somatostatin analog therapy response in patients with growth hormone-secreting pituitary macroadenomas. J Endocrinol Invest [Internet]. 2019 Apr [cited 2019 Apr 23];42(4):443–51. Available from: http://link.springer.com/10.1007/s40618-018-0939-4
72. Lang M, Habboub G, Moon D, Bandyopadhyay A, Silva D, Kennedy L, et al. Comparison of Constructive Interference in Steady-State and T1-Weighted MRI Sequence at Detecting Pituitary Adenomas in Cushing's Disease Patients. J Neurol Surg Part B Skull Base [Internet]. 2018 Dec 10 [cited 2019 Apr 23];79(06):593–8. Available from: http://www.ncbi.nlm.nih.gov/pubmed/30456030
73. Yamamoto J, Kakeda S, Shimajiri S, Takahashi M, Watanabe K, Kai Y, et al. Tumor consistency of pituitary macroadenomas: Predictive analysis on the basis of imaging

features with contrast-enhanced 3D FIESTA at 3T. Am J Neuroradiol. 2014;
74. Watanabe K, Kakeda S, Yamamoto J, Watanabe R, Nishimura J, Ohnari N, et al. Delineation of Optic Nerves and Chiasm in Close Proximity to Large Suprasellar Tumors with Contrast-enhanced FIESTA MR Imaging. Radiology [Internet]. 2012 Sep [cited 2019 Apr 23];264(3):852–8. Available from: http://www.ncbi.nlm.nih.gov/pubmed/22771880
75. Chatain GP, Patronas N, Smirniotopoulos JG, Piazza M, Benzo S, Ray-Chaudhury A, et al. Potential utility of FLAIR in MRI-negative Cushing's disease. J Neurosurg [Internet]. 2018 Sep [cited 2019 Apr 30];129(3):620–8. Available from: http://www.ncbi.nlm.nih.gov/pubmed/29027863

Table 1. Points to consider when requesting a pituitary MRI protocol

Key questions	**Options / examples**
Which sequences?	Spin Echo (SE) / Fast Spin Echo (FSE): - T1 weighted[1,2] - T2 weighted - proton density (PD) weighted[2] Gradient Echo (GE): - spoiled gradient echo (e.g. to permit thinner slices through the sella – see below) Other: - Diffusion weighted (DWI) - Perfusion weighted (PWI) - Inversion recovery (IR) - Fluid attenuation inversion recovery (FLAIR) - Magnetic resonance angiography (MRA)
With or without contrast enhancement?	Gadolinium[1]
Which planes?	Coronal; sagittal; axial
Which slice thickness?	Standard 2-3 mm; volumetric (e.g. consecutive 1 mm)
Which magnetic field strength?	1.5T, 3T, 7T

Key: [1]T1 weighted MRI following contrast may also include (i) ***dynamic sequences*** [images obtained from multiple locations throughout the gland at multiple time points (e.g. 0, 30, 60, 90, 120 and 180 seconds) to help identify microadenomas (which exhibit delayed enhancement) or distinguish residual/recurrent tumour from postoperative change], and (ii) ***delayed sequences*** (to assess the cavernous sinuses and characterize other sella/parasellar tumours); [2]Fat suppressed T1 or PD sequences may improve visualization of the posterior pituitary gland by suppressing signal from adjacent clival bone marrow.

Table 2. Specific indications for T2 weighted pituitary MRI – according to Bonneville(8)

Indication	T2 weighted MRI findings	References
Suspected microprolactinoma - potential to obviate requirement for gadolinium injection	Hyperintense	(8)
Identification of silent corticotroph macroadenomas – with differentiation from non-functioning PA	Microcystic pattern (in >50% of cases)	(8,48)
Investigation of GH-secreting PA: - prediction of response to first generation SSA therapy - identification of invasion of the medial wall of the cavernous sinus	Hypointense [commoner (>50%)]: smaller tumours with less CSI, which correspond to densely granulated tumours; good response to SSA Isointense / hyperintense: larger, typically more invasive tumours; less SSA responsive	(8,49,50)
Diagnosis of hypophysitis	Hyperintense (even when overall size of gland is within normal limits)	(8)
Diagnosis of Rathke's cleft cyst	Hypointense	(8)

Key: CSI, cavernous sinus invasion; PA, pituitary adenoma; SSA, somatostatin analogue therapy

Table 3. Alternative MR sequences that have been applied in the investigation of pituitary disorders

MRI sequence	Features	Potential application(s) in pituitary disorders	References
Diffusion weighted (DWI)	Measures the diffusion of water molecules in biological tissues; most commonly used to detect cytotoxic oedema in the context of acute cerebral ischaemia/infarction	Detection of acute pituitary apoplexy/infarction Distinguishing intra-/supra-sellar cystic lesions	(51) (52)
Apparent Diffusion Coefficient (ADC)	A subtype of DWI	Prediction of the consistency of PA pre-surgery: - some authors have reported a reduced ADC with increasing collagen content - others have found no relation between ADC and tumour consistency	(53–55) (56–58)
Diffusion Tensor (DTI)	An extension of DWI which analyses the directional diffusion of water molecules in biological tissue	Optic nerve tractography to inform treatment planning and predict likelihood of visual recovery following transsphenoidal surgery	(59–61)
Perfusion weighted (PWI)	Assesses tissue perfusion at the capillary level	Assessment of the vascularity of PA pre-surgery Identification of other vascular lesions (e.g. meningioma) which may be mistaken for a PA	(62) (63,64)
Magnetic Resonance Angiography (MRA)	Provides detailed images of the arterial system	Detection of intrasellar aneurysms Delineation of cranial nerves in their cavernous sinus segment	(65) (66)

Magnetic Resonance Elastography (MRE)	Measures the propagation of shear waves through tissue of interest to provide an estimate of stiffness	Inform surgical planning by estimating whether a PA is likely to be soft (and suckable), or intermediate or firm (requiring curettage for resection)	(67)
Magnetic Resonance Spectroscopy (MRA)	Provides information on metabolic function through the measurement of different metabolites (e.g. acetylaspartate, choline, creatine)	Differentiation of PA from normal gland Differential diagnosis of suprasellar lesions Predicting response of somatotroph tumours to SSA therapy	(68) (69,70) (71)
Balanced steady state free precession (e.g. Constructive Interference in Steady State, CISS; Fast Imaging Employing Steady-state Acquisition Cycled phases, FIESTA-C)	Image contrast determined by T2/T1 ratio of the tissue; in practice, heavily water weighted (good contrast between CSF and other structures) but also sensitive to contrast enhancement	Improved detection of adenoma in Cushing disease Improved evaluation of cavernous sinus invasion Prediction of adenoma consistency Improved delineation of optic nerves and chiasm in large pituitary tumors	(72) (72) (73) (74)
Fluid Attenuation Inversion Recovery (FLAIR)	An inversion recovery sequence with a long inversion time that removes signal from the CSF which is therefore dark rather than bright as would normally be seen on T2 sequences	In Cushing disease, delayed contrast washout from a corticotroph microadenoma may be detected as FLAIR hyperintensity	(75)

Key: PA, pituitary adenoma; SSA, somatostatin analogue therapy

Figure legends

Fig. 1 Normal pituitary MRI. **a-d** Spin Echo (SE) T1 weighted coronal and sagittal sequences (pre- and post-gadolinium enhancement). **e,f** Fast Spin Echo (FSE) T2 weighted coronal and axial sequences. ***Key:*** Gad, gadolinium; ic-ICA, intracavernous segment of the internal carotid artery; Inf, infundibulum; OC, optic chiasm; PP, posterior pituitary gland; sc-ICA, supracavernous segment of the internal carotid artery; SpS, sphenoid sinus.

Fig. 2 Spectrum of pituitary adenomas. **a** Left-sided microadenoma exhibiting delayed contrast enhancement (yellow arrow). **b** macroadenoma, displacing the pituitary stalk and normal remaining gland to the left (white arrow); there is only limited suprasellar extension (without compression of the optic chiasm), but clear extension in to the right cavernous sinus (yellow arrow). **c** macroadenoma with marked suprasellar extension compressing the optic chiasm (left>right) (dotted yellow arrows) and right parasellar extension (yellow arrow). **d** macroadenoma with suprasellar extension resulting in compression of the optic chiasm (dotted yellow arrows) and left parasellar extension (yellow arrow) – Knosp grade 3A (white dashed line); the remaining normal gland is seen on the right/superiorly (white arrow). ***Key:*** Gad, gadolinium; T1 SE, T1 weighted Spin Echo MRI.

Fig. 3 Pituitary CT. **a,b** Macroprolactinoma with extensive right parasellar and suprasellar extension, and involvement of the skull base (yellow arrows); the position of the optic chiasm (yellow dotted arrows) and infundibulum (white arrow) are shown. **c** Intrasellar calcification (yellow arrows) in a patient with a thyrotroph adenoma.

Fig. 4 Confirmation of suspected microprolactinoma using ^{11}C-methionine PET. **a** Indeterminate coronal T1 weighted gadolinium enhanced SE MRI in a 22-year-old female with bilateral galactorrhoea, secondary amenorrhoea and moderate hyperprolactinaemia (PRL 3.8 × upper limit of normal), confounded by antipsychotic medication usage. **b,c** Post-gadolinium

FSPGR MRI in coronal and axial planes identifies a possible right-sided microadenoma (yellow arrows). **d,e** ^{11}C-methionine PET/CT coregistered with FSPGR MRI confirms the site of the suspected microprolactinoma (yellow arrows). ***Key:*** FSPGR, Fast Spoiled Gradient Recalled Echo; Gad, gadolinium; PRL, prolactin; SE, Spin Echo.

Fig. 5 Confirmation of site of suspected residual somatotroph adenoma using ^{11}C-methionine PET. **a** T1 weighted gadolinium enhanced SE MRI in a 50-year-old female with persistent acromegaly following transsphenoidal surgery (IGF-1 1.9 $\times$ upper limit of normal); poorly enhancing tissue can be seen medial and inferior to the right cavernous sinus (yellow arrows), with normal enhancing tissue on the left of the sella (white arrow). **b,c** Post-gadolinium FSPGR MRI in coronal and axial planes confirms an area of poorly enhancing tissue on the right of the sella possibly extending in to the right cavernous sinus (yellow arrows). **d,e** ^{11}C-methionine PET/CT coregistered with FSPGR MRI demonstrates focal tracer uptake in the right side of the sella, but without cavernous sinus extension (yellow arrows); note low level tracer uptake is also seen in the residual normal pituitary tissue (white arrow). ***Key:*** FSPGR, Fast Spoiled Gradient Recalled Echo; Gad, gadolinium; IGF-1, insulin-like growth factor 1; SE, Spin Echo.

Fig. 6 Identification of a left-sided corticotroph adenoma using ^{11}C-methionine PET. **a** Indeterminate T1 weighted gadolinium enhanced SE MRI in a 32-year-old female with Cushing disease; there is minor inferior deviation of the floor of the sella on the left (yellow arrow), but no clear adenoma is seen. **b** bilateral inferior petrosal sinus sampling shows clear central:peripheral (>245:1 at 3 min) and right:left (>145:1 at 3 min) ACTH (ng/L) gradients following injection of 100 mcg human CRH **c,d** Post-gadolinium FSPGR MRI in coronal and axial planes fails to identify a definite adenoma. **d,e** ^{11}C-methionine PET/CT coregistered with FSPGR MRI demonstrates focal tracer uptake in the left side of the gland (yellow arrows); at surgery a left-sided corticotroph adenoma was resected with resultant hypocortisolism. ***Key:***

CRH, corticotrophin releasing hormone; FSPGR, Fast Spoiled Gradient Recalled Echo; Gad, gadolinium; L, left; P, peripheral; R, right; SE, Spin Echo.

Fig. 7 Identification of a right-sided thyrotroph adenoma using ^{11}C-methionine PET. **a** Indeterminate T1 weighted gadolinium enhanced SE MRI in a 62-year-old female with a biochemically confirmed thyrotropinoma; no clear adenoma is seen. **b,c** Post-gadolinium FSPGR MRI in coronal and axial planes raises suspicion of a possible abnormality on the right side of the sella (yellow arrows), but no definite adenoma is seen. **d,e** ^{11}C-methionine PET/CT coregistered with FSPGR MRI demonstrates intense focal tracer uptake in the right side of the gland (yellow arrows); at surgery a right-sided thyrotroph adenoma was resected with complete resolution of hyperthyroxinaemia secondary to inappropriate TSH secretion. ***Key:*** FSPGR, Fast Spoiled Gradient Recalled Echo; Gad, gadolinium; SE, Spin Echo.

Fig. 8 Confirmation of the site of recurrent gonadotropinoma using ^{11}C-methionine PET. **a** T1 weighted gadolinium enhanced SE MRI in a 50-year-old male with a recurrent functioning FSH-secreting pituitary adenoma; abnormal tissue is seen in the left sella region with extension in to the sphenoid sinus (yellow arrows), but it is difficult to be sure whether this all represents recurrent disease as opposed to post-operative change; the pituitary stalk and normal gland are displaced to the right (white arrow) . **b,c** Post-gadolinium FSPGR MRI in coronal and axial planes confirms the findings on SE sequences. **d,e** ^{11}C-methionine PET/CT coregistered with FSPGR MRI demonstrates focal tracer uptake predominantly by tissue in the sphenoid sinus with only modest sella uptake (yellow arrows); the normal gland shows low level uptake of 11C-methionine (white arrow). ***Key:*** FSPGR, Fast Spoiled Gradient Recalled Echo; Gad, gadolinium; SE, Spin Echo.

Figure 9: Absent ^{11}C-methionine uptake in a pituitary cyst. **a** T1 weighted gadolinium enhanced SE MRI in a 74-year-old female with an incidentally detected right-sided pituitary cystic lesion (yellow arrow); the normal gland is seen on the left (white arrow). **b,c** Post-

gadolinium FSPGR MRI in coronal and axial planes confirms the findings on SE sequences. **d,e** ^{11}C-methionine PET/CT coregistered with FSPGR MRI demonstrates low level tracer uptake only in the normal gland (white arrows). ***Key:*** FSPGR, Fast Spoiled Gradient Recalled Echo; Gad, gadolinium; SE, Spin Echo.

Bashari et al - Figure 1

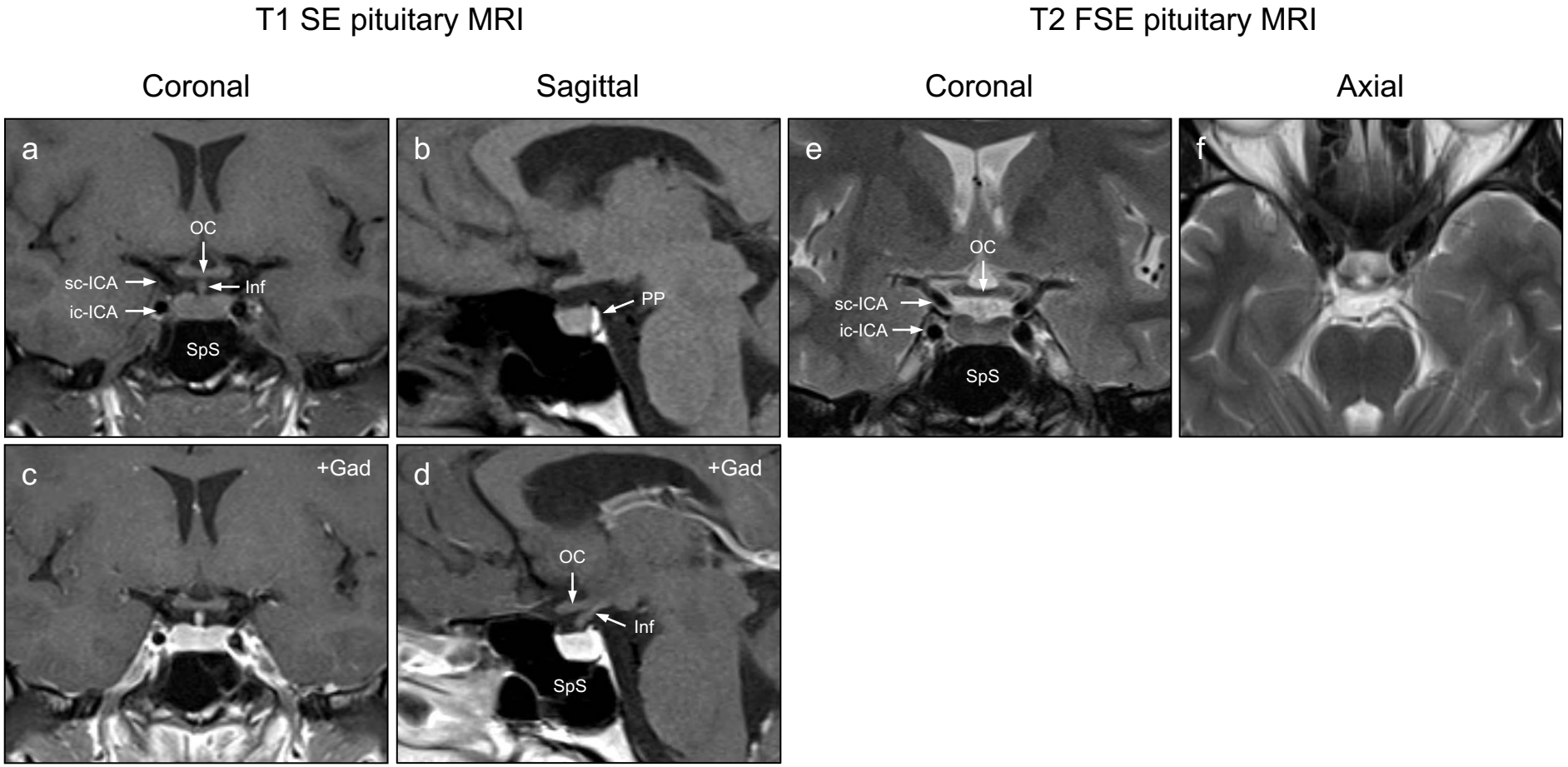

T1 SE pituitary coronal MRI

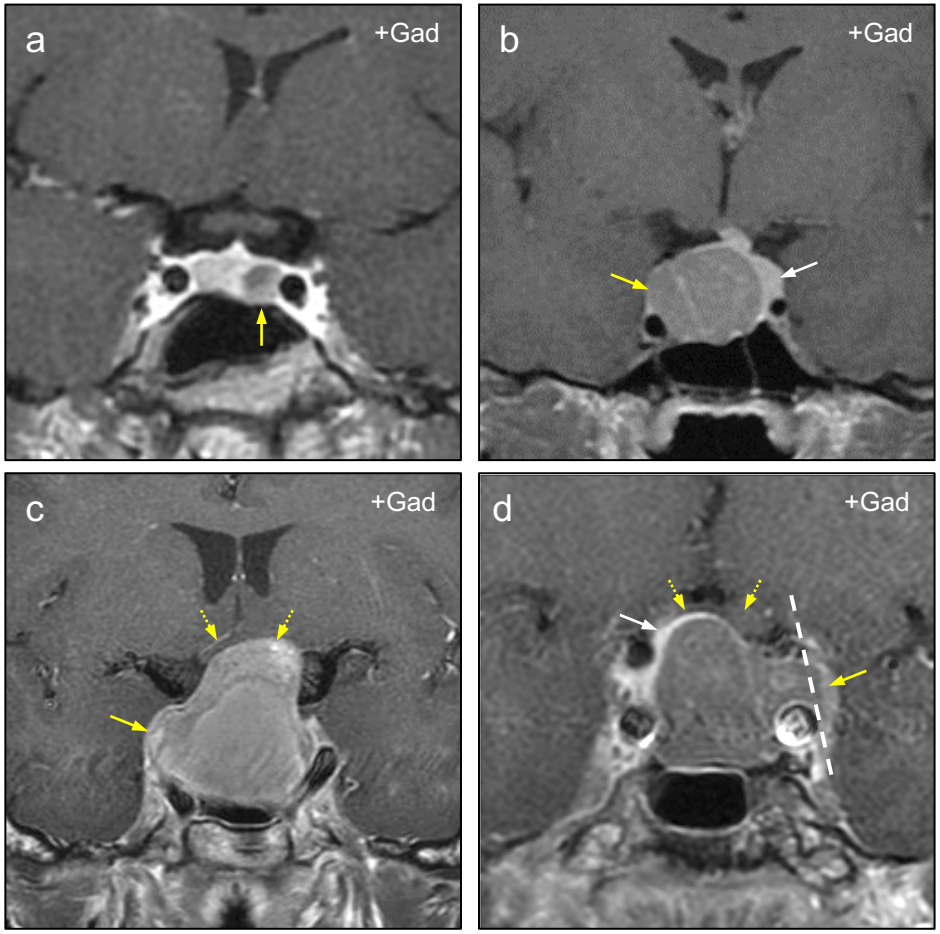

CT pituitary

Coronal

Axial

Axial

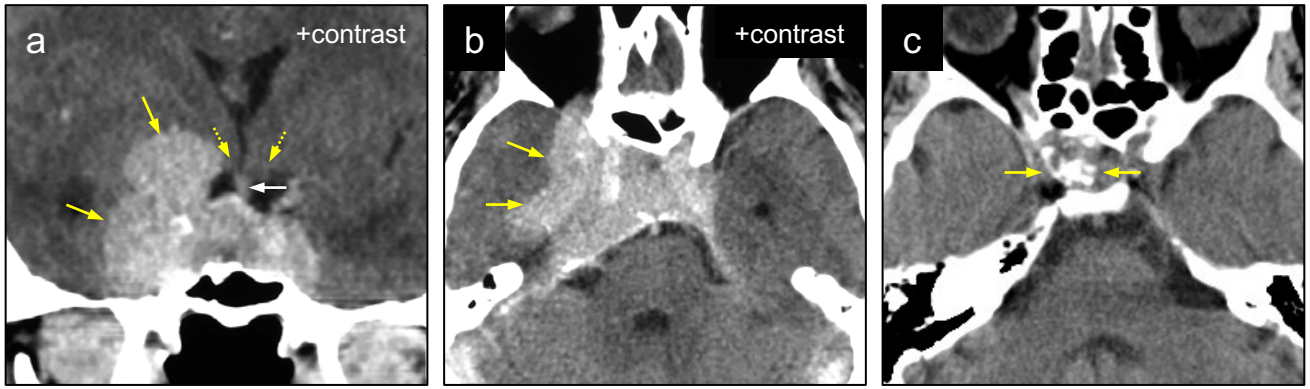

Bashari et al - Figure 4

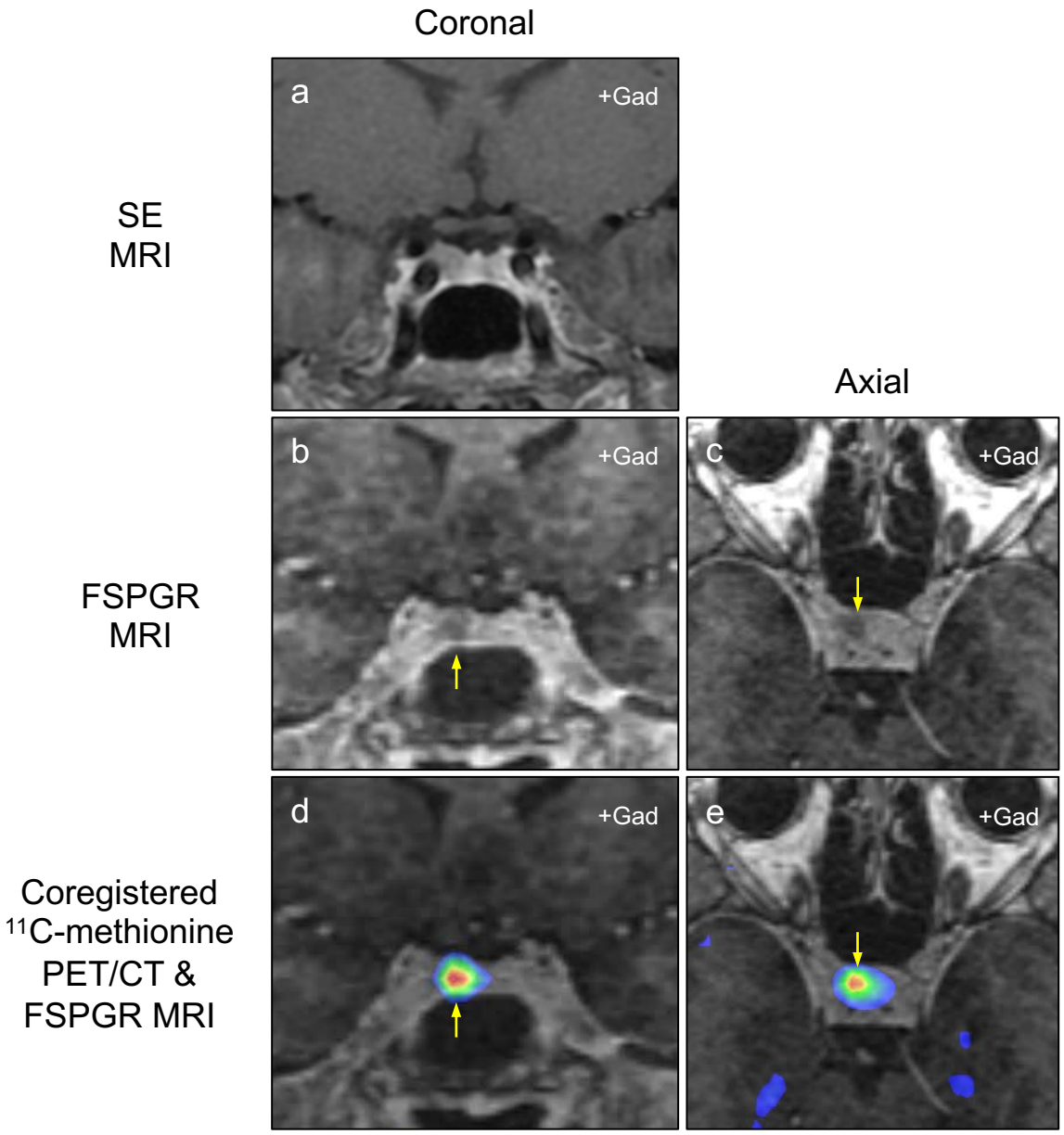

Bashari et al - Figure 5

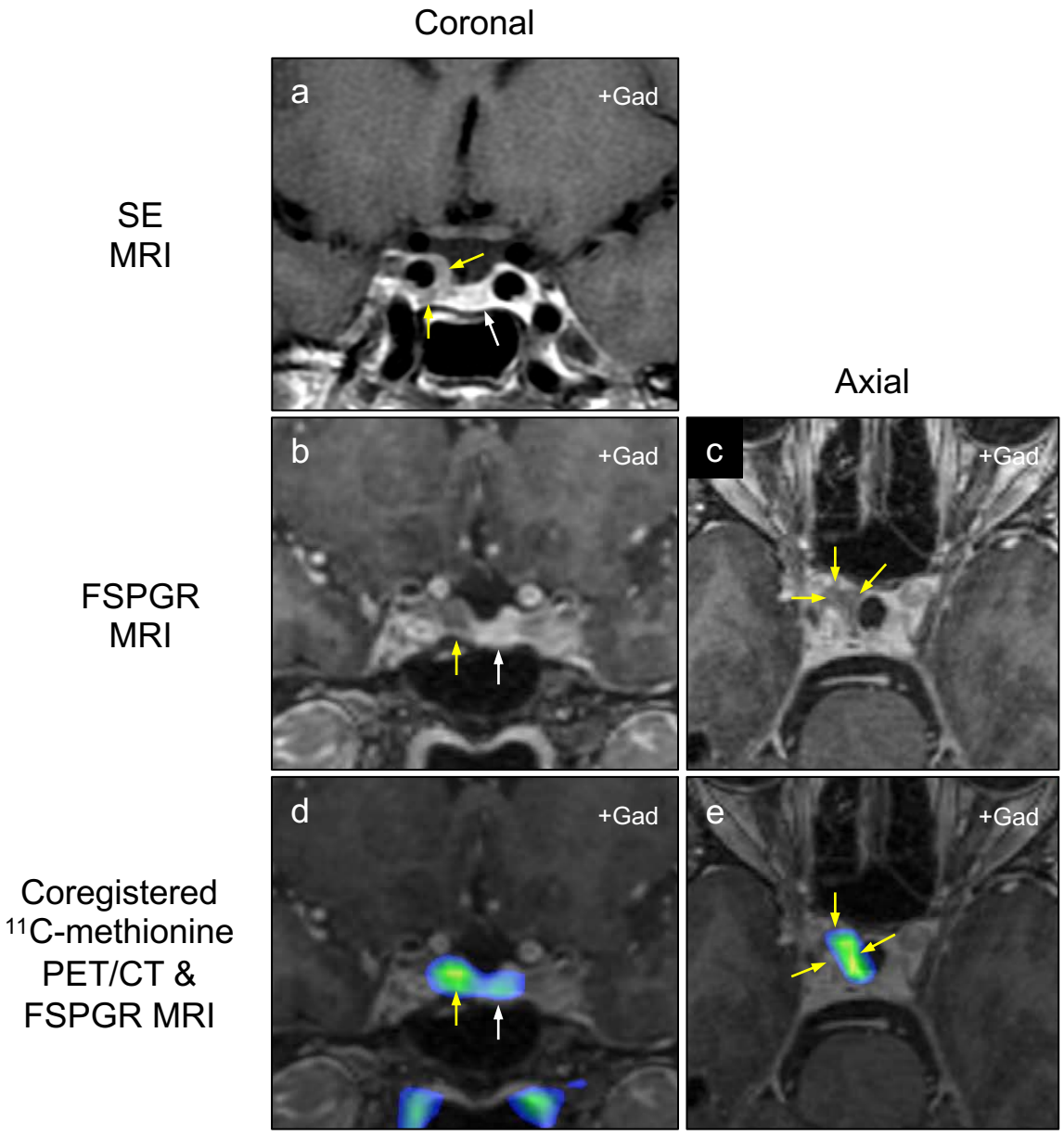

Bashari et al - Figure 6

Coronal

Axial

SE MRI

FSPGR MRI

Coregistered ^{11}C-methionine PET/CT & FSPGR MRI

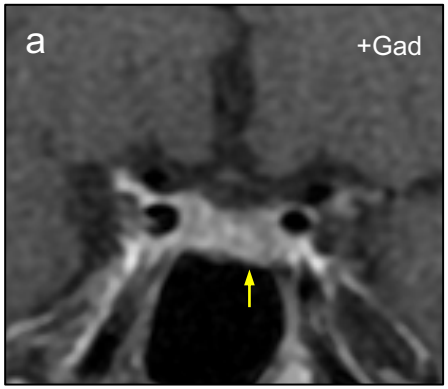

b

IPSS ACTH	Midnight cortisol 537 nmol/L (<50)		
Time	R	L	P
Basal 1	380	20	19
Basal 2	314	20	19
1 min	3630	28	16
3min	8349	57	34
10 min	4788	143	114

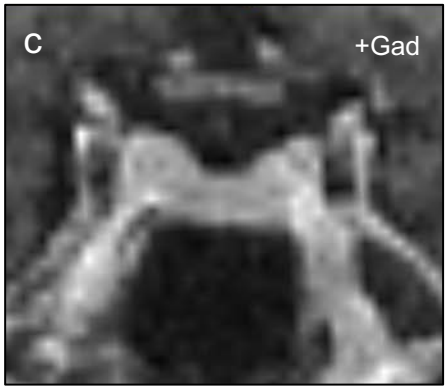

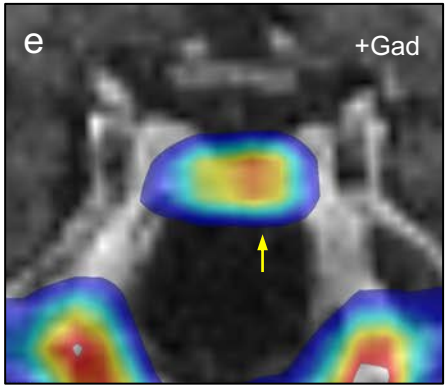

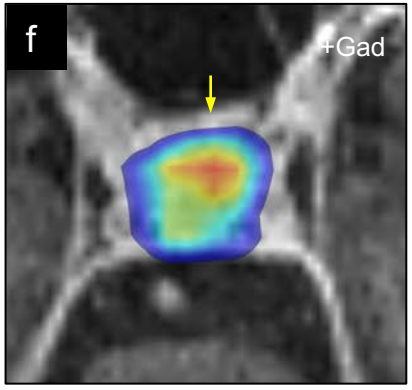

Bashari et al - Figure 7

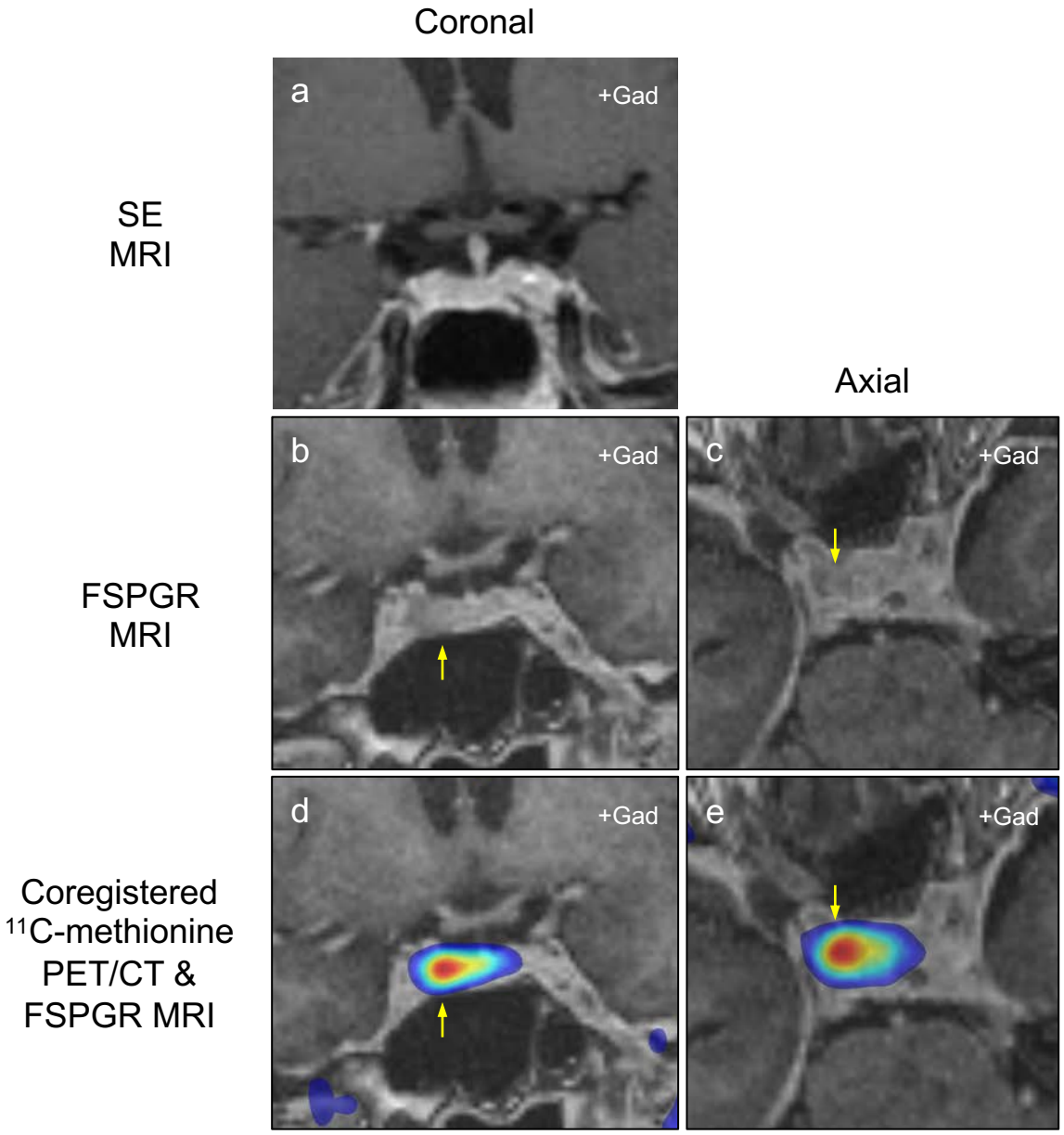

Bashari et al - Figure 8

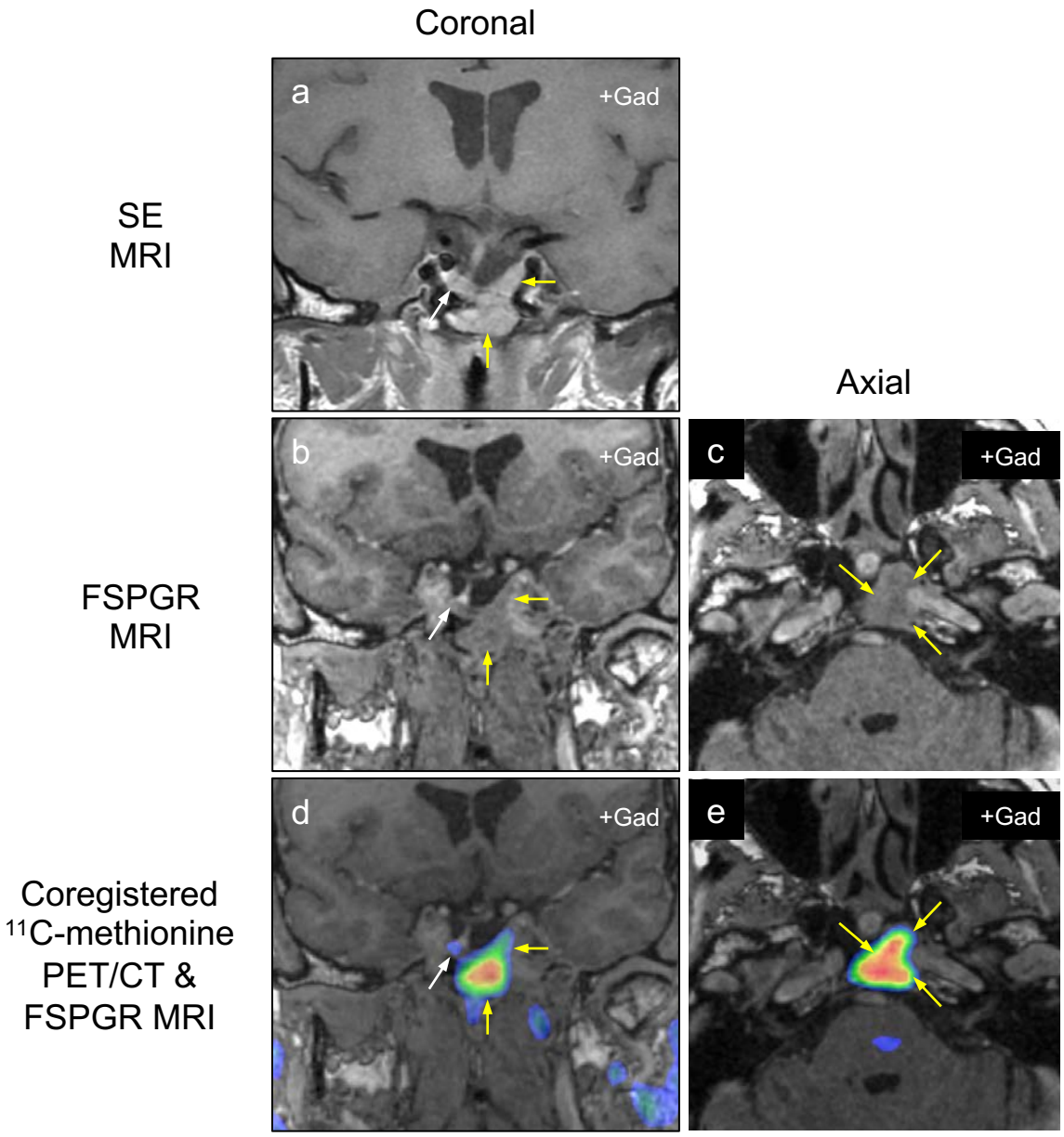

Bashari et al - Figure 9